

Original Article

Cite this article: Arar Y, Dimas VV, Nugent AW, Hussain T, Kasraie N, Reddy SRV, Zellers TM, and Herbert C (2022) Pre-procedural CT imaging aids neonatal PDA stenting for ductal-dependent pulmonary blood flow with reduction in overall procedural morbidity. *Cardiology in the Young* **32**: 1401–1406. doi: [10.1017/S1047951121004133](https://doi.org/10.1017/S1047951121004133)

Received: 1 August 2021
 Revised: 6 September 2021
 Accepted: 19 September 2021
 First published online: 19 October 2021



Keywords:

Congenital heart Disease; paediatric catheterisation/intervention; advanced imaging; cardiac CT

Author for correspondence:

Y. Arar, Pediatric Cardiology, Department of Pediatrics, UT Southwestern Children's Medical Center, 1935 Medical District Drive, Dallas, TX 75235-7701, USA. Tel: +214 456 7311; Fax: +214 456 6154.
 E-mail: Yousef.Arar@UTSouthwestern.edu

Pre-procedural CT imaging aids neonatal PDA stenting for ductal-dependent pulmonary blood flow with reduction in overall procedural morbidity

Yousef Arar^{1,2} , V. Vivian Dimas^{1,2}, Alan W. Nugent³, Tarique Hussain^{1,2}, Nima Kasraie⁴, Surendranath R. Veeram Reddy^{1,2} , Thomas M. Zellers^{1,2} and Carrie Herbert^{1,2}

¹Department of Pediatrics, University of Texas Southwestern Medical Center, Dallas, Texas, USA; ²Pediatric Cardiology, Children's Medical Center, Dallas, Texas, USA; ³Department of Pediatrics, Division of Pediatric Cardiology, Ann & Robert H. Lurie Children's Hospital of Chicago, Chicago, Illinois, USA and ⁴Department of Radiology, University of Texas Southwestern Medical Center, Dallas, Texas, USA

Abstract

Patent ductus arteriosus stenting for ductal-dependent pulmonary blood flow is a technically challenging neonatal procedure to maintain a stable pulmonary circulation. Pre-procedural computed tomography imaging aids in outlining ductal origin, insertion, size, course and curvature. Computed tomography imaging may add value to procedural outcomes and reduce overall procedural morbidity in neonatal patent ductus arteriosus stenting. We conducted a single centre retrospective chart review of neonates with ductal-dependent pulmonary blood flow who underwent patent ductus arteriosus stenting between January 1, 2014 and June 31, 2020. We compared patients variables between patients who underwent pre-procedural computed tomography imaging to those who did not. A total of 64 patients were referred for patent ductus arteriosus stenting with 33 (52%) obtaining pre-procedural computed tomography imaging. Average age [19 days; range 1–242 days ($p = 0.85$)] and weight [3.3 kg (range 2.2–6.0 kg; $p = 0.19$)] was not significantly different between the groups. A diagnosis of pulmonary atresia was made in 42 out of 64 (66%) patients prior to patent ductus arteriosus stenting. The cohort with pre-intervention computed tomography imaging had a significant reduction in the total number of access sites (1.2 versus 1.5; $p = 0.03$), contrast needed (5.9 versus 8.2 ml/kg; $p = 0.008$), fluoroscopy (20.7 versus 38.8 minutes; $p = 0.02$) and procedural time (83.4–128.4 minutes; $p = 0.002$) for the intervention. There was no significant difference in radiation burden between the groups ($p = 0.35$). Pre-procedural computed tomography imaging adds value by aiding interventional planning for neonatal patent ductus arteriosus stenting. A statistically significant reduction in the number of access sites, contrast exposure, as well as fluoroscopic and procedural time was noted without significantly increasing the cumulative radiation burden.

Introduction

Patent ductus arteriosus stenting represents a viable alternative to surgical shunts for initial short-term palliation of neonates with critical congenital heart disease in need of stable postnatal pulmonary circulation.¹ Patent ductus arteriosus stenting for ductal-dependent pulmonary blood flow is a technically challenging neonatal procedure to maintain a stable pulmonary circulation. Pre-procedural planning with cross-sectional imaging for patent ductus arteriosus stenting in a neonate with ductal-dependent pulmonary blood flow using computed tomography has been previously described.^{2,3} Patent ductus arteriosus morphology for stenting have also been previously described as straight (type 1), “mildly” tortuous with one turn (type 2) and very tortuous with >1 turn (type 3).³ Some consider type 3 ducts not amenable for stenting but others have found procedure times and need for multiple stents did not differ based on patent ductus arteriosus type or ductal tortuosity index.³

Planning vascular access in order to deliver the patent ductus arteriosus stent in the straightest trajectory is a fundamental part in the success of the procedure.⁴ In mid-2018, a routine pre-procedural computed tomography imaging prior to patent ductus arteriosus stenting was implemented at our institution for ductal-dependent pulmonary blood flow lesions with the initial goal of better understanding the optimal access site. The objective is to determine if pre-procedural computed tomography scanning added value by improved success or by reducing the number of access sites attempted, by reducing procedural time, contrast volume, fluoroscopy time and adverse events.

Materials and methods

This study was a retrospective chart review of all neonates with ductal-dependent pulmonary blood flow referred to the catheterisation lab for patent ductus arteriosus stenting at Children's Medical Center in Dallas, Texas, between January 1, 2014 and June 31, 2020. Neonatal patent ductus arteriosus stenting as a method of palliating patients with ductal-dependent pulmonary blood flow was started in high-risk cases in 2011. By 2014, it was established as the primary method for all patients and with the interventionalists' learning curve completed.

Institutional Review Board at UT Southwestern Medical Center approval was obtained for retrospective analysis of patient data. Patient demographic information as well as pre-catheterisation imaging and catheterisation data was collected. Pre-procedural imaging was performed via a 256-slice Dual Source Siemens SOMATOM Flash computed tomography (Siemens Healthcare, Munich, GR). Interventional procedures were performed in a Phillips Alluraclarity (Philips Healthcare, Best, NL) or Siemens Q.zen (Siemens Healthcare, Munich, GR) biplane fluoroscopy lab. Radiation burden estimates were calculated using previously accepted dose conversion coefficients and k-factor coefficients.⁵⁻⁸ Radiation conversion coefficients for biplane fluoroscopy (0.26)⁷ and computed tomography (0.026)⁸ were used to estimate the overall exposure in millisieverts. All other statistical methods were done using GraphPad Prism software (Graph Pad Software Inc., version 9) including Chi-square test and paired t-test.

This study included only those patients referred for patent ductus arteriosus stenting for ductal-dependent pulmonary blood flow lesions. Patients who underwent concomitant interventions were excluded to avoid confounding results. Neonates with ductal-dependent systemic blood flow were also excluded. No neonates with ductal-dependent pulmonary blood flow were excluded based on patient demographics, genetics, anatomy or prior intervention. The assigned attending interventionalist for the case determined the need for pre-procedural computed tomography imaging and not necessarily determined by transthoracic echocardiogram's assessment of ductal tortuosity and/or suggestion of the need for non-traditional access sites (carotid artery, axillary artery, etc.). Unlike previously published work on this subject,² no 3D reconstructed models were printed for any of these cases; however, 3D volume rendering of computed tomography images was routinely performed. All computed tomography procedures were performed using a single high-pitched helical (FLASH) acquisition with angiography triggered manually with the region of interest in the descending aorta. All computed tomography procedures were performed free breathing and without sedation.

If deemed necessary by the interventionalist, prostaglandins were stopped prior to transfer to the catheterisation lab to allow for decreased intraluminal ductal diameter, thus facilitating stent placement with appropriate apposition. All procedures were performed with the patient intubated and mechanically ventilated. The majority of patients underwent percutaneous access with United States of America guidance; however, surgical carotid artery cutdown was performed on selected patients at the interventionalist's discretion.

The basic procedure involved first obtaining vascular access with stable sheath position followed by a pre-intervention angiogram to establish landmarks. After review of angiography, a wire was advanced across the patent ductus arteriosus followed by stent placement. In some cases, a microcatheter or double wire technique was used to further aid the process. Bare metal coronary,

non-drug eluting stents were used in the majority of patients (62/66 = 94%) during this study period. All patients were continued on heparin for 72 hours. Outpatient anticoagulation therapy post procedure was based on interventionalist preference with at least aspirin prescribed.

After successful stent deployment, all patients were transferred to our cardiac intensive care unit for observation with follow-up echocardiogram performed to establish a new baseline.

Results

A total of 77 patients with ductal-dependent pulmonary blood flow were referred to the catheterisation lab for patent ductus arteriosus stenting. All patients had a transthoracic echocardiogram performed prior to referral. Thirteen patients were excluded from this study based on additional catheter-based interventions at the time of patent ductus arteriosus stenting (pulmonary valve radiofrequency ablation, ductus venosus stenting for obstructed TAPVR and right ventricular outflow tract stent). Of the remaining 64 patients, 31 (48%) had no pre-intervention computed tomography imaging and 33 (52%) presented to the catheterisation lab with pre-intervention computed tomography imaging (Table 1) to aid with vascular access planning. Average age [19 days; range 1–242 days ($p = 0.85$)] and weight [3.3 kg; range 2.2–6.0 kg ($p = 0.19$)] were not significantly different between the two groups. A diagnosis of pulmonary atresia was made in 42 out of 64 (66%) patients prior to patent ductus arteriosus stenting. Access site used for stent deployment is outlined in Table 2 as follows: left carotid artery 14 (22%), left axillary artery 13 (20%), right carotid artery 11 (17%), right femoral artery 10 (16%), left femoral artery 7 (11%), right femoral vein 7 (11%), and left femoral vein 2 (3%). Total patient radiation burden is outlined in Table 3 based on previously accepted dose conversion coefficients and k-factor coefficients^{7,8} to best estimate the effective radiation dose in millisieverts. Total radiation burden for patients who did not receive pre-procedural computed tomography imaging was not significantly different than those who did have cardiac cross-sectional imaging (0.92 versus 1.07 millisieverts, respectively ($p = 0.35$)). Case examples of the most common approaches are outlined in Figure 1. Of those patients who underwent carotid artery approach ($n = 25$), percutaneous carotid artery access was utilised in 68% ($n = 17$) and surgical carotid artery cutdown was utilised in 32% ($n = 8$).

Out of 77 cases, 2 (3%) patent ductus arteriosus were not amenable to stenting because of extreme tortuosity (type 3 patent ductus arteriosus, ductal tortuosity index ~450; Fig 5) and large size of the patent ductus arteriosus. Out of the 64 patients included in our study, there were 13 (20%) procedure-related complications including stent migration/embolisation ($n = 4$; 6%), need for blood transfusion due to significant blood loss ($n = 4$; 6%), significant hypotension requiring epinephrine ($n = 2$; 3%), patent ductus arteriosus thrombus ($n = 1$; 2%), carotid artery pseudoaneurysm ($n = 1$; 2%) and carotid artery dissection ($n = 1$; 2%). No procedure-related mortalities occurred. Of note, 85% (11/13, $X^2 = 8.5$, $p = 0.003$) of the complications listed occurred in patients who did not receive pre-procedural computed tomography imaging. The complications were evenly distributed across the study time period.

A comparison of patients with and without pre-procedural computed tomography imaging is further outlined in Table 1. Pre-procedural computed tomography imaging led to a significant reduction in the average total number of access sites (1.2 versus 1.5; $p = 0.03$), contrast needed (5.9 versus 8.2 ml/kg;

Table 1. Demographic and procedural data comparing the two groups of PDA-stented patients with and without pre-procedural cardiac CT imaging. There is a statistically significant reduction in the total number of access sites, contrast needed, fluoroscopic and procedural sheath time for the intervention

	n = 64 Overall	n = 33 (52%) CT patients	n = 31 (48%) No CT patients	
Age at Cath (days)	19 ± 15.2	18 ± 14.3	20 ± 16.1	p = 0.85
Weight at Cath (kg)	3.3 ± 0.6	3.2 ± 0.6	3.4 ± 0.6	p = 0.19
Number of access sites	1.3 ± 0.6	1.2 ± 0.5	1.5 ± 0.6	p = 0.03
Contrast (ml/kg)	7 ± 3.2	5.9 ± 2.4	8.2 ± 3.9	p = 0.008
Fluoro time (minute)	29.5 ± 30.5	20.7 ± 17.3	38.8 ± 36.0	p = 0.02
Sheath time (minute)	105.2 ± 59.6	83.4 ± 49.3	128.4 ± 63.8	p = 0.002

Table 2. Summary of access sites used for PDA stent deployment

PDA access site for intervention	
Left carotid artery (LCA)	14
Left axillary artery (LAM)	13
Right carotid artery (RCA)	11
Right femoral artery (RFA)	10
Left femoral artery (LFA)	7
Right femoral vein (RFV)	7
Left femoral vein (LFV)	2
Total	64

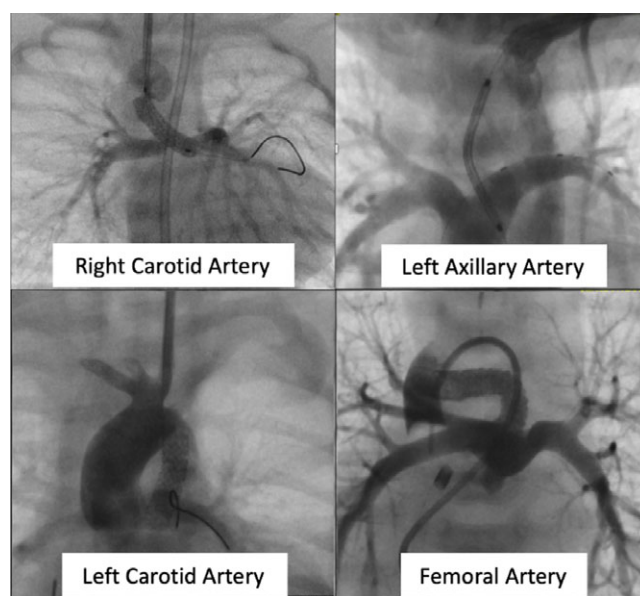
Table 3. Summary of radiation burden comparing the two groups of PDA stented patients with and without pre-procedural cardiac CT imaging

n = 31 (48%)	n = 33 (52%)	
Fluoro only patients (mSv)	Fluoro + CT patients (mSv)	p-value
Biplane-fluoroscopy		
0.92 ± 1.8	0.54 ± 0.2	0.1
CT		
n/a	0.53 ± 0.6	n/a
Cumulative radiation		
0.92 ± 1.8	1.07 ± 0.47	0.35

p = 0.008), fluoroscopic (20.7 versus 38.8 minutes; p = 0.02) and procedural sheath time (83.4–128.4 minutes; p = 0.002) for the intervention. Examples of the procedures are summarised in Figure 2 (left axillary artery) and Figure 3 (left carotid artery). Furthermore, Figure 4 shows the difficulties when attempting to stent a significantly tortuous type 3 patent ductus arteriosus that does not straighten after traversing with a wire and stent.

Discussion

With the growing body of literature supporting the short- and long-term benefits of patent ductus arteriosus stenting,^{9–12} focus is rightly shifting toward improving morbidity associated with the procedure. To our knowledge, this is the first study evaluating outcomes related to pre-procedural computed tomography imaging for pulmonary-dependent patent ductus arteriosus stenting. Patent ductus arteriosus stenting is a procedure that requires meticulous pre-interventional planning and real-time operator

**Figure 1.** Case examples of the most common vascular access sites used for PDA stent deployment.

resourcefulness. Appropriate infrastructure and skillset are imperative to allow for the multiple approaches necessary for successfully performing complex ductal stenting. With increased utilisation of pre-procedural cross-sectional imaging and planning, we have seen a dramatic shift in the ease of the procedure (less access sites, contrast use, and procedural/fluoroscopic time) as well as the reduction in patient complications.

Innovative indications for computed tomography imaging are emerging rapidly in the congenital cardiac population to help plan and direct interventions. A recent intraclass correlation coefficient study was performed to compare pre-procedural computed tomography imaging to selective catheter angiograms for ductal dimensions.¹³ Overall, there was moderate agreement between pre-intervention straight (intraclass correlation coefficient = 0.68) and actual (intraclass correlation coefficient = 0.65) lengths for computed tomography versus fluoroscopy. Interestingly, the group also showed poor agreement (intraclass correlation coefficient = 0.39) when comparing patent ductus arteriosus straight fluoroscopic length measurements pre- and post-stent placement. This discrepancy shows that ductal morphology, tortuosity and reactivity vary tremendously from patient to patient and pre- to post-stenting. Further work is needed to understand the relationship between pre-procedural modelling and ductal reactivity during this procedure.

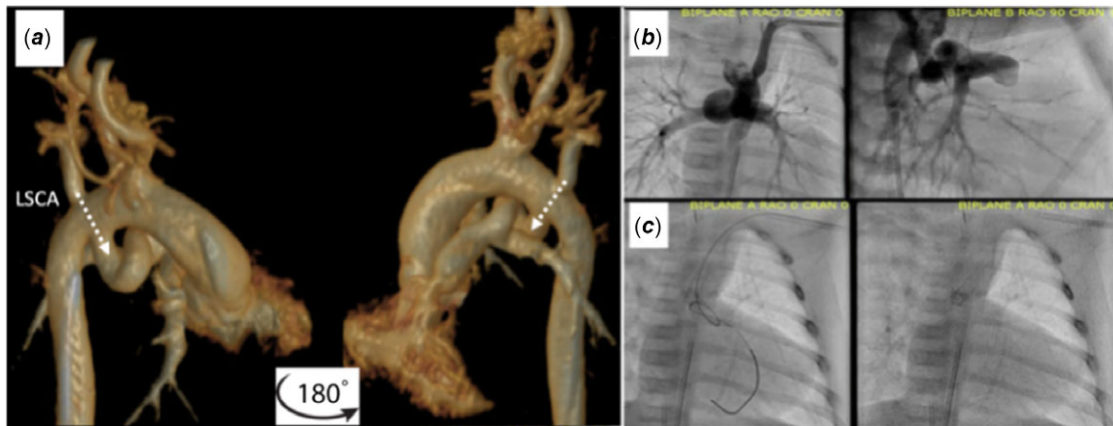


Figure 2. Neonatal PDA stenting approach and procedure. (a) Pre-procedural cardiac CT 3D reconstruction showing a “corkscrew” PDA. (b) Patient was approached via the left axillary artery (LAA) to left subclavian artery (LSCA) for PDA stenting. (c) Successful delivery of a 3.5 mm × 23 mm Vision Multilink stent.

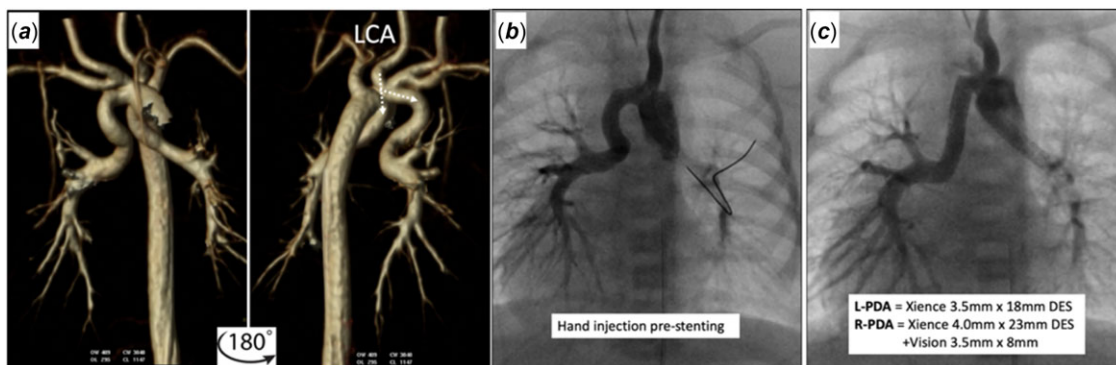


Figure 3. Neonate with discontinuous pulmonary arteries and bilateral PDAs. (a) Pre-procedural cardiac CT 3D reconstruction shows the left carotid artery (LCA) as the best approach to stent both PDAs via one access site. (b and c) Both PDAs are stented via the LCA. One stent [Xience 3.5 mm × 18 mm drug eluting stent (DES)] was placed in the left PDA and two stents were placed in the right PDA (Xience 3.5 mm × 18 mm DES × 1 and 3.5 mm × 8 mm Vision Multilink stent × 1).

Unlike previously published reports,² we elected to utilise only 3D reconstructed volume-rendered images rather than 3D-printed models. The decision to 3D print may be institutional-dependent, but we found 3D printing added unnecessary delay with minimal additional procedural planning value.

The significant improvements in fluoroscopy time and contrast reduction are likely due to pre-procedural planning. As noted above, there was no use of 3D models, and only one case utilised overlay¹⁴ guidance. Not surprisingly, in this case, there was significant distortion from the wire after crossing the patent ductus arteriosus, limiting the effectiveness of the overlay. The pre-procedural computed tomography assists in choosing the best access site with the most direct line to the duct, which leads to technically easier and more efficient patent ductus arteriosus crossing. The more direct line also makes stent delivery over the wire, often a challenge in tortuous ducts, more successful. The fluoroscopic camera detector angles to outline the aortic and PA ends of the patent ductus arteriosus with angiography are also known before the case, which leads to shorter and more efficient procedures.

Further investigation is needed for factors that may predict patent ductus arteriosus that are not amenable to stenting. In our single centre study, increased ductal tortuosity index in type 3 patent ductus arteriosus was associated with the increased difficulty of the procedure. This was most evident when the patent ductus arteriosus would not straighten when crossed with a wire, as seen in

Figure 5. Due to the limited number of patients with this ductal configuration in our cohort, we are not able to comment on the direct relationship at this time. Future studies will look at the relationship of ductal tortuosity index, patent ductus arteriosus straightening with wire across, and a ratio of ductal tortuosity index to the patent ductus arteriosus measured length from the anterior to posterior dimension. It is not currently recommended to stent if patent ductus arteriosus tortuosity remains despite attempts to straighten with equipment. Anecdotally, this increases the difficulty of the procedure and likelihood of stent embolisation.

This was a retrospective review of a single centre’s experience with patent ductus arteriosus stenting using pre-procedural computed tomography scans. The majority of patients with pre-intervention computed tomography imaging included the latter half of the cohort. This may arguably bias the results as the interventionalists gained even more experience with the procedure and have a better understanding of ideal patent ductus arteriosus stenting outcomes. However, we elected to exclude the first several years of ductal stenting experience to, at least partially, account for the learning curve.

Comparing total effective ionising radiation dose between patients who had pre-procedural computed tomography imaging and those who were only exposed via biplane fluoroscopy is important. It was a challenge to accurately report this value due to the different units used between the two modalities [(computed

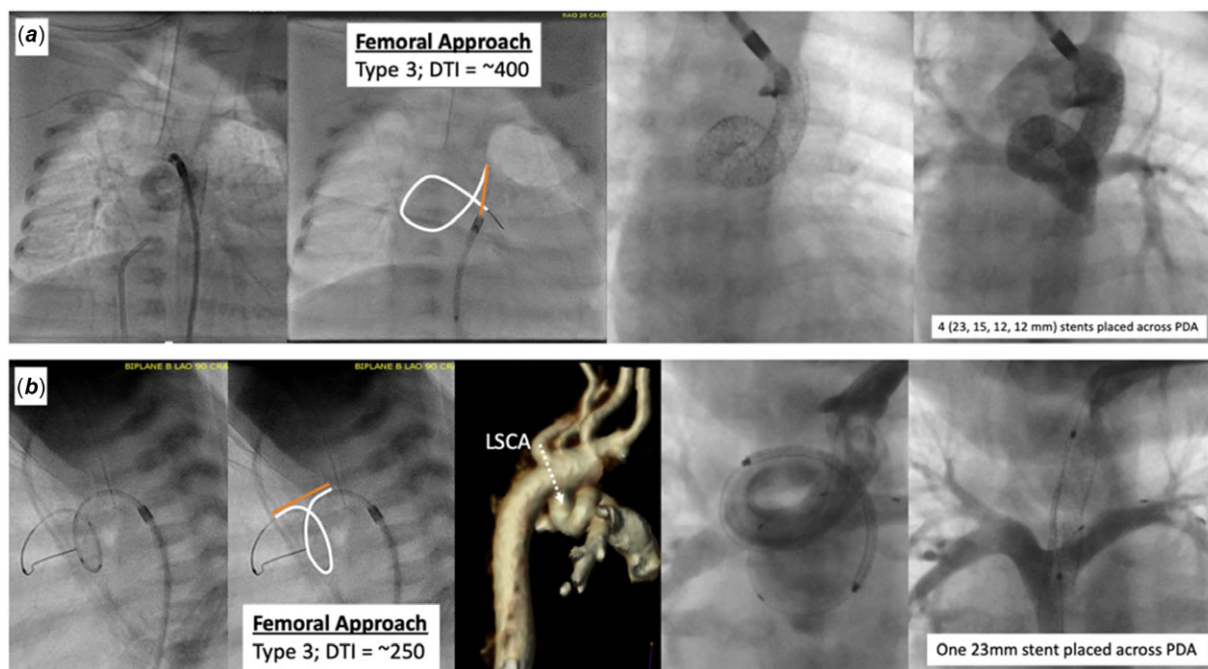


Figure 4. Series of images showing difficulties when stenting a tortuous PDA that does not straighten after traversing with a wire/stent. (a) Upper panel starts with a hand injection at the aortic end of the PDA from the femoral approach showing a type 3 PDA with a ductal tortuosity index (DTI) of approximately 400. The wire and stent would not advance from the femoral approach so a right carotid artery approach was attempted. Notice that the PDA did not straighten out and multiple stents (3.5 mm × 23, 14, 12, 12 mm Vision Multilink stents) were required to traverse the full length of the tortuous PDA. (b) Lower panel shows another example of a tortuous PDA unsuccessfully approached from the femoral artery (type 3; DTI ~250). In this example, the patient was re-approached via the left axillary artery to the left subclavian artery (LSCA) and the PDA straightened out with wire and stent across. This delivery was made much simpler because of the straightening of the PDA with only one long stent required (3.5 mm × 23 mm Vision Multilink). Orange line = Straight PDA length; White (solid) line = Actual PDA length; White (dashed) line = Ideal site of access for PDA stenting virtually represented on CT 3D reconstruction.

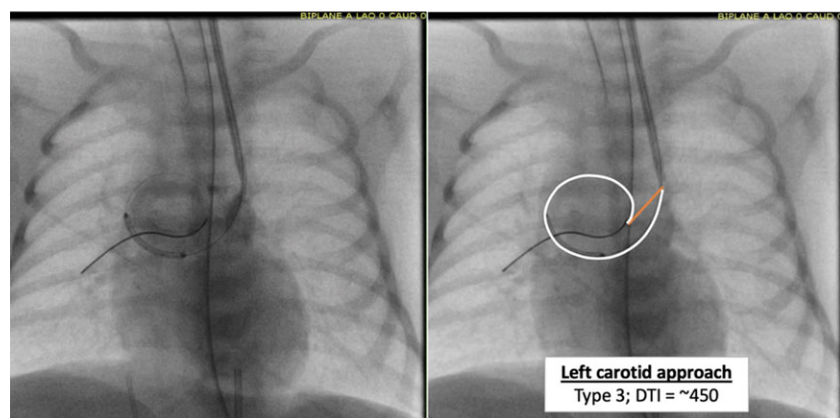


Figure 5. Neonate with an extremely tortuosity type 3 PDA with a ductal tortuosity index of approximately 450. Despite appropriate vascular access planning, the stent is not able to overcome the tortuosity of the PDA. This patient was referred for a modified Blalock–Taussig shunt directly from the catheterisation lab. Orange line = straight PDA length; white line = actual PDA length.

tomography = dose length product = milligray × centimetre (mGy*cm); biplane fluoroscopy = dose area product = microgray × metres² (μGy*m²)). Based on our best estimates, there was no significant difference between the biplane fluoroscopy only patients (no computed tomography) and those who received a pre-procedural computed tomography for patent ductus arteriosus stent planning (p = 0.35, Table 3). We continue to work with the radiation physicist at our institution to understand the best prospective design to compare these important variables for future studies, as we recognise the importance of cumulative radiation exposure on neonates.

Furthermore, each interventionalist was allowed autonomy with each case. The request for pre-procedural computed tomography imaging and/or chosen access site was on an individual basis

without necessarily requiring group consensus. Due to variability in practice pre- and post-intervention, there may be an unknown element of individual bias in an approach that cannot be accurately quantified. A total of five different attending interventionalists performed the procedures in this study.

Conclusion

Pre-procedural computed tomography imaging aids interventional planning for neonatal patent ductus arteriosus stenting for ductal-dependent pulmonary blood flow with reduction in overall procedural morbidity. A statistically significant reduction in the number of access sites, contrast exposure, as well as fluoroscopic and procedural time was noted without

significantly increasing the cumulative radiation burden. Future studies are needed to assess the overall radiation burden for patients who have a computed tomography versus those who go to the catheterisation lab with no cross-sectional imaging. With continued advances in cross-sectional imaging, we plan to further analyse patent ductus arteriosus characteristics to predict those that are not amenable to stenting.

Acknowledgements. The authors would like to thank the cardiac catheterisation and advanced imaging staff at Children's Medical Center Dallas.

Financial support. No additional funding was needed for this clinically indicated retrospective study.

Conflicts of interest. None.

Ethical standards. The authors assert that all procedures contributing to this work comply with the ethical standards of the U.S. Good Clinical Practice Guidelines and with the Helsinki Declaration of 1975, as revised in 2008, and has been approved by the institutional review board of UT Southwestern – STU 2019-1628.

References

- Gibbs JL, Rothman MT, Rees MR, Parsons JM, Blackburn ME, Ruiz CE. Stenting of the arterial duct: a new approach to palliation for pulmonary atresia. *Br Heart J* 1992; 67: 240–245.
- Chamberlain RC, Ezekian JE, Sturgeon GM, Barker PCA, Hill KD, Fleming GA. Preprocedural three-dimensional planning aids in transcatheter ductal stent placement: a single-center experience. *Catheter Cardiovasc Interv* 2020; 95(6): 1141–1148. DOI [10.1002/ccd.28669](https://doi.org/10.1002/ccd.28669).
- Qureshi AM, Goldstein BH, Glatz AC, et al. Classification scheme for ductal morphology in cyanotic patients with ductal dependent pulmonary blood flow and association with outcomes of patent ductus arteriosus stenting. *Catheter Cardiovasc Interv* 2019; 93(5): 933–943. DOI [10.1002/ccd.28125](https://doi.org/10.1002/ccd.28125). Epub 2019 Feb 21.
- Aggarwal V, Petit CJ, Glatz AC, Goldstein BH, Qureshi AM. Stenting of the ductus arteriosus for ductal-dependent pulmonary blood flow—current techniques and procedural considerations. *Congenit Heart Dis* 2019; 14: 110–115. DOI [10.1111/chd.12709](https://doi.org/10.1111/chd.12709).
- Romanyukha A, Folio L, Lamart S, Simon SL, Lee C. Body size-specific effective dose conversion coefficients for CT scans. *Radiat Prot Dosimetry* 2016; 172: 428–437. DOI [10.1093/rpd/ncv511](https://doi.org/10.1093/rpd/ncv511).
- Deak PD, Smal Y, Kalender WA. Multisection CT protocols: sex- and age-specific conversion factors used to determine effective dose from dose-length product. *Radiology* 2010; 257: 158–166. DOI [10.1148/radiol.10100047](https://doi.org/10.1148/radiol.10100047).
- Schauer DA, Linton OW. NCRP Report No. 160, Ionizing Radiation Exposure of the Population of the United States, medical exposure—are we doing less with more, and is there a role for health physicists? *Health Phys* 2009; 97: 1–5. DOI [10.1097/01.HP.0000356672.44380.b7](https://doi.org/10.1097/01.HP.0000356672.44380.b7).
- Trattner S, Halliburton S, Thompson CM, et al. Cardiac-specific conversion factors to estimate radiation effective dose from dose-length product in computed tomography. *JACC Cardiovasc Imaging* 2018; 11: 64–74. DOI [10.1016/j.jcmg.2017.06.006](https://doi.org/10.1016/j.jcmg.2017.06.006).
- Nicholson GT, Glatz AC, Qureshi AM, et al. Impact of palliation strategy on interstage feeding and somatic growth for infants with ductal-dependent pulmonary blood flow: results from the congenital catheterization research collaborative. *J Am Heart Assoc* 2020; 9: e013807. DOI [10.1161/JAHA.119.013807](https://doi.org/10.1161/JAHA.119.013807).
- Glatz AC, Petit CJ, Goldstein BH, et al. A comparison between patent ductus arteriosus stent and modified Blalock-Taussig shunt as palliation for infants with ductal-dependent pulmonary blood flow: insights from the congenital catheterization research collaborative. *Circulation* 2018; 137: 581–588.
- Bentham JR, Zava NK, Harrison WJ, et al. Duct stenting versus modified Blalock Taussig shunt in neonates with duct-dependent pulmonary blood flow: associations with clinical outcomes in a multicenter national study. *Circulation* 2018; 137: 589–601.
- Roggen M, Cools B, Brown S, et al. Can ductus arteriosus morphology influence technique/outcome of stent treatment? *Catheter Cardiovasc Interv* 2020; 95: 1149–1157. DOI [10.1002/ccd.28725](https://doi.org/10.1002/ccd.28725).
- Jadhav SP, Aggarwal V, Madand PM, Diaz E, Zhang W, Qureshi AM. Correlation of ductus arteriosus length and morphology between computed tomographic angiography and catheter angiography and their relation to ductal stent length. *Pediatr Radiol* 2020; 50: 800–809. DOI [10.1007/s00247-020-04624-1](https://doi.org/10.1007/s00247-020-04624-1).
- Arar Y, Reddy SRV, Kim H, et al. 3D advanced imaging overlay with rapid registration in CHD to reduce radiation and assist cardiac catheterisation interventions. *Cardiol Young* 2020; 30(5): 656–662. DOI [10.1017/S1047951120000712](https://doi.org/10.1017/S1047951120000712). Epub 2020 Apr 15.